J. Quant. Spectrosc. Radiat. Transfer. Vol. 13, pp. 601–613. Pergamon Press 1973. Printed in Great Britain

FREE–FREE RADIATION IN ELECTRON-NEUTRAL ATOM COLLISIONS

SYDNEY GELTMAN*

Joint Institute for Laboratory Astrophysics, University of Colorado, Boulder, Colorado 80302, U.S.A.

(*Received* 15 *November* 1972)

Abstract—Free–free absorption coefficients are calculated for the electron-neutral atom systems involving He, C, N, O, Ne, Ar, Kr and Xe. The calculations are based upon model atomic potentials which have been adjusted to fit experimental scattering cross sections or electron affinities. Some angular distributions are presented and thermal averages are evaluated in the ranges $\lambda = 0.5$–$20\ \mu$m and $T = 500$–$20{,}000°$K.

1. INTRODUCTION

A FREE electron undergoing a collision with an atomic system emits or absorbs continuous radiation as a result of its acceleration in the atomic field. A photon is emitted (bremsstrahlung) or absorbed (inverse bremsstrahlung) while the incident electron loses or gains the corresponding amount of kinetic energy. The large atomic mass allows us to neglect recoil energies in the atomic system. Our present concern is with low energy electrons (< 10 eV) and photons (visible and infrared).

For fully-ionized plasmas, the important bremsstrahlung encounters are between electrons and positive ions, while, for somewhat lower temperature gases such as those occurring in stellar atmospheres, the main source of bremsstrahlung is electron-neutral atom collisions. In the electron-positive ion case, the dynamics of the collision is dominated by the long-range Coulomb attraction, and the Sommerfeld–Maue result[1,2] for an unscreened Coulomb field is a good first-order approximation. The effects of departures from the pure Coulomb field have been studied with the quantum defect method by PEACH.[3]

In the electron-neutral atom case the absence of a dominant Coulomb field makes the free–free transition rate extremely sensitive to the details of the short-range interaction. We no longer have an analytical first-order approximation with which to estimate these cross sections and we are dependent upon numerical calculations on each of the atomic constituents of interest. In astrophysical applications the dominant atom is hydrogen, and most theoretical work has been concentrated on that system.[4–8] Interest in the continuous emission of radiation from hot air has led to theoretical studies on nitrogen and oxygen atoms.[9–11] The role of free–free transitions in the continuous spectra of excited gases is discussed in the review paper of BIBERMAN and NORMAN,[12] and the role in astrophysics is covered in the review of MYERSCOUGH and PEACH.[13]

* Staff Member, Laboratory Astrophysics Division, National Bureau of Standards.

2. THEORY

(a) *General formulae*

In a complete theoretical description of the free–free transitions of an electron colliding with an n-electron atom, one would first require solutions of the elastic scattering problem and then calculate dipole matrix elements with these $(n+1)$-electron wave functions. As this procedure is impractical in all except the smallest atoms we adopt the simplification that the atom can be represented by an effective spherically symmetric potential. This simplification has been used successfully to describe elastic scattering and photodetachment,[14,15] and we would expect it to give comparable accuracy in a free–free calculation.

The differential cross section for the absorption of a photon $\hbar\omega$ by an electron of initial wave vector $\mathbf{k}_i$ resulting in the final wave vector $\mathbf{k}_f$ is given by

$$\frac{d\sigma_{ab}}{d\Omega_f} = \frac{e^2 m}{2\pi\hbar^2 c}\omega k_f |\langle f|\hat{\boldsymbol{\varepsilon}}\cdot\mathbf{r}|i\rangle|^2 \tag{1}$$

where $\hat{\boldsymbol{\varepsilon}}$ is the electric field polarization unit vector, and $|i\rangle$ and $|f\rangle$ are the continuum states $\psi^+_{\mathbf{k}_i}$ and $\psi^-_{\mathbf{k}_f}$. The partial wave expansion of the continuum states is

$$\psi^{\pm}_{\mathbf{k}}(\mathbf{r}) = \sum_{l=0}^{\infty} i^l(2l+1)\,e^{\pm i\eta_l}\frac{u_l(k,r)}{kr}P_l(\hat{\mathbf{k}}\cdot\hat{\mathbf{r}}), \tag{2}$$

where η_l is the scattering phase shift and $u_l(k,r)$ is the radial wave function satisfying

$$\left[\frac{d^2}{dr^2} - \frac{l(l+1)}{r^2} - U(r) + k^2\right]u_l = 0, \tag{3}$$

having asymptotic form $u_l \to \sin(kr - l\pi/2 + \eta_l)$. Our choices of potential $U(r)$ will be discussed in the next section. Thus, for a given $\hat{\boldsymbol{\varepsilon}}$ and $U(r)$, the above differential cross section will be a function of $\mathbf{k}_i$, $\hat{\mathbf{k}}_f$, and ω, with energy conservation requiring $\hbar^2(k_f^2 - k_i^2)/2m = \hbar\omega$.

The dimensions of the above differential cross section are cm^5/sr since the normalization used for the continuum wave functions corresponds to unit electron density. One would get the usual dimensions of cm^2/sr after multiplying by the electron density in the incident electron beam. A total free–free absorption cross section is obtained by integrating (1) over $d\Omega_f$, and one may also average over all directions of incident electrons to obtain

$$\sigma_{ab}(k_i,\omega) = \frac{1}{4\pi}\int\int d\Omega_i\, d\Omega_f \frac{d\sigma_{ab}}{d\Omega_f}. \tag{4}$$

This quantity is independent of the polarization vector since all other directions have been integrated over, and hence it applies to both polarized or unpolarized light.

The free–free emission (bremsstrahlung) cross section may be defined in terms of the absorption cross section by means of

$$\hbar\omega\sigma_{em}(k_f,\omega) = \frac{m}{\pi^2\hbar}\frac{k_i^2}{k_f^2}\frac{\omega^3}{k_i c^2}\sigma_{ab}(k_i,\omega). \tag{5}$$

Here σ_{em} is a cross section per unit energy of the emitted photon, so each side of (4) has the dimensions of cm^2. For application to the study of the continuum absorption by hot gases

it is useful to define a mean absorption coefficient as the Maxwell average of σ_{ab},

$$\kappa(\lambda, T) = \int \mathrm{d}\mathbf{v}_i f(v_i, T)\sigma_{ab}(k_i, \omega), \tag{6}$$

where f is the normalized Maxwell distribution for the electrons. This quantity still has the dimensions of cm^5 and corresponds to an atomic absorption coefficient per unit electron density. The emission properties are generally described in terms of a volume emission coefficient,

$$\mathscr{E}(T) = \frac{1}{4\pi}\int \mathrm{d}\mathbf{v}_f v_f f(v_f, T)\int \mathrm{d}(\hbar\omega)\hbar\omega\sigma_{em}(k_f, \omega), \tag{7}$$

where the lower limit of v_f is given by $\frac{1}{2}mv_f^2 = \hbar\omega$. An emissivity per unit wavelength, $J(\lambda, T)$, may also be defined, where

$$\mathscr{E}(T) = \int_0^\infty \mathrm{d}\lambda J(\lambda, T). \tag{8}$$

The emissivity J thus describes the rate of emission of power per unit wavelength into unit solid angle from a volume containing unit electron and atom densities. It follows that $J(\lambda, T)$ can be expressed in terms of $\kappa(\lambda, T)$ by means of relations (5)–(8).

We return now to the evaluation of the basic microscopic quantity, $\mathrm{d}\sigma_{ab}/\mathrm{d}\Omega_f$, from which may be obtained all of the above defined macroscopic coefficients. For the geometry in which $\mathbf{k}_i$ is parallel to the direction of linear polarization $\hat{\boldsymbol{\varepsilon}}$, the modulus square of the matrix element is given by

$$\begin{aligned}|\langle f|\hat{\boldsymbol{\varepsilon}}\cdot\mathbf{r}|i\rangle|^2 = \frac{1}{\pi^4 k_i^2 k_f^2}\sum_{ll'} \mathrm{e}^{i[\eta_l(i)-\eta_{l'}(i)]}\cdot\\ \cdot\{ll'\,\mathrm{e}^{i[\eta_{l-1}(f)-\eta_{l'-1}(f)]}R^L_{l-1\,l}R^L_{l'-1\,l'}P_{l-1}P_{l'-1}\\ -l(l'+1)\,\mathrm{e}^{i[\eta_{l-1}(f)-\eta_{l'+1}(f)]}R^L_{l-1\,l}R^L_{l'+1\,l'}P_{l-1}P_{l'+1}\\ -l'(l+1)\,\mathrm{e}^{i[\eta_{l+1}(f)-\eta_{l'-1}(f)]}R^L_{l+1\,l}R^L_{l'-1\,l'}P_{l+1}P_{l'-1}\\ +(l+1)(l'+1)\,\mathrm{e}^{i[\eta_{l+1}(f)-\eta_{l'+1}(f)]}R^L_{l+1\,l}R^L_{l'+1\,l'}P_{l+1}P_{l'+1}\},\end{aligned} \tag{9}$$

where $\eta_l(i, f)$ refers to phase shift at initial or final energies, the argument of the Legendre polynomials is $\hat{\mathbf{k}}_i\cdot\hat{\mathbf{k}}_f$, and the length form of the radial matrix element is

$$R^L_{l_f l_i} = \int_0^\infty \mathrm{d}r u_{l_f}(k_f, r) r u_{l_i}(k_i, r).$$

As is well known, the following identity relates the length, velocity and acceleration forms of the dipole matrix element, respectively:

$$im\omega\langle f|\hat{\boldsymbol{\varepsilon}}\cdot\mathbf{r}|i\rangle = \frac{\hbar}{i}\langle f|\hat{\boldsymbol{\varepsilon}}\cdot\nabla|i\rangle = \frac{i}{2\omega}\langle f|\hat{\boldsymbol{\varepsilon}}\cdot\nabla U|i\rangle. \tag{10}$$

It will be more convenient to use the acceleration form of the radial matrix element,

$$R^A_{l_f l_i} = \int_0^\infty \mathrm{d}r u_{l_f}(k_f, r) \frac{\mathrm{d}U}{\mathrm{d}r} u_{l_i}(k_i, r),$$

than the length form, since $\mathrm{d}U/\mathrm{d}r$ is a short-range function and the above integral is immediately convergent. From (10), we have

$$R^L_{l_f l_i} = \frac{1}{2m\omega^2} R^A_{l_f l_i}.$$

Carrying out the angular integrals in (4) using (9), one has

$$\sigma_{ab}(k_i, \omega) = \frac{\alpha}{3\pi^4} \frac{k_f}{k_i^2 k_f^2 (\Delta k^2)^3} \sum_l \{l |R^A_{l-1\,l}|^2 + (l+1)|R^A_{l+1\,l}|^2\}, \tag{11}$$

where α is the fine structure constant and $\Delta k^2 = k_f^2 - k_i^2$.

(b) *Atomic model*

The atomic potential that we use in the present calculations is the one used by ROBINSON and GELTMAN[15] in the evaluation of photodetachment cross sections. It has the form

$$U(r) = U_{HS}(r) + \frac{2}{r}(1 - \mathrm{e}^{-r/r_0}) - \alpha \frac{(1 - \mathrm{e}^{-r/r_p})}{(r_p^2 + r^2)^2}, \tag{12}$$

where U_{HS} is the Hartree–Fock–Slater potential for the neutral atom (seen by an atomic electron) as evaluated by the methods of HERMAN and SKILLMAN,[16] where the second term removes the Coulomb tail contained in U_{HS}, and where the third term is a polarization potential. The detailed functional forms for the last two terms were chosen to insure that they vanished as $r \to 0$, since in that limit the correct potential is given by U_{HS}, and to go as $2/r$ and $-\alpha/r^4$ in the $r \to \infty$ limit.

The values adopted for the atomic polarizability α are the best presently available from theory or measurement.[17] This leaves the two parameters, r_0 and r_p, free for adjustment to match other known properties.

In their study of photodetachment of negative ions, Robinson and Geltman assigned values for r_p and then adjusted r_0 to give a binding energy in agreement with the known electron affinities. We will adopt this procedure for C and O. For the rare gas atoms, there exist considerable electron scattering data, both total and momentum transfer cross sections.[18] We have adjusted both r_p and r_0 to give optimum agreement with the scattering data in the energy range < 10 eV. The quality of these fits is quite good, with our optimum calculated cross section generally falling within the scatter of the measurements. The energies of the calculated Ramsauer minima in Ar, Kr and Xe are found to be within 10 per cent of their measured values. The largest relative discrepancy in these fits occurs in the magnitude of the cross section at the Ramsauer minimum for Kr and Xe, where the measurements are about one-half of the calculated value. This indicates an error of about 30 per cent in the small p-wave phase shifts at these energies. For the N atom, which does not have a positive electron affinity in its ground state and for which only meager scattering

data are available, we have used an interpolated value for the r_0 parameter based on its values for C and O. The non-existence of the ground state negative ion N^- is due to the relatively high lying position of the expected ^3P term, rather than any irregularity in the effective central potential of N as compared with its neighbors C and O.

The potential parameters adopted by the above procedures are listed in Table 1 and the corresponding elastic scattering cross sections are given in Table 2. Since these cross sections are largely found by fitting to data, this table may be used as a convenient reference source for workers needing these cross sections. The values in Table 2 for O are slightly different from those in Ref. (15) because partial waves up to $l = 4$ have been included, and similarly for C because an improved value for the polarizability has become available. Although the potential parameters for O have been determined on the basis of its electron affinity, the resulting elastic scattering cross section is in excellent agreement with the measurements of SUNSHINE *et al.*[19] and about 50 per cent above the measurements of NEYNABER *et al.*[20] Similarly, our elastic scattering results for N are about 50 per cent above the measurements of Neynaber *et al.*

TABLE 1. OPTIMUM POTENTIAL PARAMETERS

Atom	$\alpha(a_0^3)$	$r_p(a_0)$	$r_0(a_0)$
Helium	1.383	0.50	0.40
Carbon	11.8	1.50	1.254
Nitrogen	7.62	1.50	1.176
Oxygen	5.19	1.50	1.098
Neon	2.663	0.85	0.80
Argon	11.08	2.50	1.60
Krypton	16.73	3.50	1.95
Xenon	27.29	4.50	2.30

3. RESULTS

There has been considerable discussion in the literature[20–24] on the use of asymptotic approximations for continuum wave functions which allows the free–free absorption coefficient to be expressed in terms of elastic scattering cross sections. Such a relation is strictly valid only in the limit of $\Delta k^2/k_i^2 \to 0$. We have made some model calculations based on a square-well potential to test the validity of these asymptotic approximations for larger values of $\Delta k^2/k_i^2$. Our general conclusion is that extension of the Low theorem[21] is often justified for potentials which are so weak as to not have any bound states, but not justified when the potential becomes strong enough for binding. In the case of the present atoms the existence of electron affinities and Ramsauer minima means that the potentials are strong enough to maintain bound states, and hence the use of asymptotic approximations would be questionable. Thus all of our numerical work here is done without approximation. The quantities defined in the preceding section have been evaluated by obtaining numerical solutions of the radial Schrödinger equation for $u_l(k, r)$, numerically evaluating the integrals for $R^A_{l_f l_i}$, and constructing the appropriate sums over l.

(a) *Angular distributions*

To date no measurements have been possible on the angular distribution of electrons following free–free absorption, but the increasing availability of high power lasers and techniques for electron energy resolution could make such direct measurements possible

TABLE 2. CALCULATED ELASTIC SCATTERING CROSS SECTIONS (IN 10^{-16} cm^2)

	$k^2a_0^2$													
	0.005	0.01	0.02	0.03	0.05	0.07	0.09	0.11	0.15	0.19	0.23	0.3	0.4	0.5
He	5.90	6.06	6.21	6.28	6.32	6.30	6.24	6.17	6.00	5.82	5.64	5.34	4.97	4.65
C	1.06	1.93	3.32	4.44	6.25	7.63	8.70	9.52	10.7	11.4	11.8	12.2	12.5	12.7
N	1.23	1.87	2.86	3.68	5.03	6.07	6.87	7.50	8.38	8.92	9.25	9.53	9.64	9.64
O	1.19	1.62	2.26	2.78	3.64	4.33	4.89	5.34	6.02	6.48	6.78	7.09	7.25	7.30
Ne	0.660	0.844	1.10	1.28	1.55	1.74	1.89	2.01	2.21	2.36	2.47	2.63	2.80	2.93
Ar	1.86	0.809	0.330	0.453	1.11	1.86	2.61	3.34	4.69	5.90	6.98	8.61	10.5	12.3
Kr	14.2	7.50	2.78	1.37	1.10	1.81	2.83	3.95	6.21	8.34	10.3	13.2	16.6	19.5
Xe	32.1	15.6	5.70	3.17	2.92	4.43	6.50	8.75	13.3	17.5	21.3	27.2	34.1	38.7

in the near future.[25] Thus it is of interest to look in detail at the angular distributions our present calculations would predict. Let us assume a geometry as shown in Fig. 1 in which an atom beam is crossed by a laser beam and a monochromatic electron beam. We take the laser beam to be linearly polarized with electric polarization vector perpendicular to the atom beam and parallel to the incident electron beam. Then the angular distribution of electrons which have undergone a free–free absorption is given by (9). The corresponding differential cross section is given in Table 3 for the heavier rare gases, an incident electron energy of 5 eV, and for the two laser wavelengths, $\lambda = 10.6\ \mu m$ (CO_2) and $\lambda = 1.06\ \mu m$ (Neodymium-glass). We also give for reference the differential cross sections for pure elastic scattering. It is necessary in a measurement to discriminate between the elastically scattered electrons and those which have absorbed a photon, and the ratio of these currents into any given element of solid angle is

$$\frac{\Delta N_{\text{elast}}}{\Delta N_{ab}} = \frac{v_e}{j_p}\frac{V_{ea}}{V_{eap}}\frac{(d\sigma_{\text{elast}}/d\Omega)}{(d\sigma_{ab}/d\Omega)}, \tag{13}$$

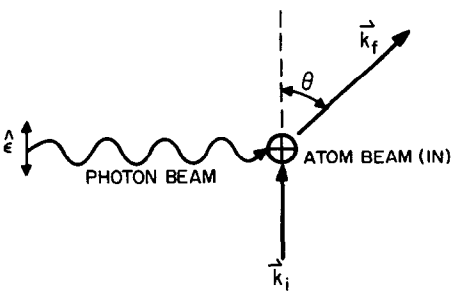

FIG. 1. Geometry of possible free–free absorption experiment corresponding to calculated quantities in Table 3.

TABLE 3. DIFFERENTIAL CROSS SECTIONS FOR FREE–FREE ABSORPTION PER UNIT ELECTRON DENSITY (IN cm^5/sr)* AT WAVELENGTHS 1.06 AND 10.6 μm AND ELASTIC SCATTERING OF ELECTRONS (IN 10^{-16} cm^2/sr). INCIDENT ELECTRON ENERGY IS 5 eV

	Ar			Kr			Xe		
$\cos\theta$	$\frac{d\sigma_{ab}}{d\Omega}$		$\frac{d\sigma_{\text{elast}}}{d\Omega}$	$\frac{d\sigma_{ab}}{d\Omega}$		$\frac{d\sigma_{\text{elast}}}{d\Omega}$	$\frac{d\sigma_{ab}}{d\Omega}$		$\frac{d\sigma_{\text{elast}}}{d\Omega}$
	$\lambda = 1.06$	$\lambda = 10.6$		$\lambda = 1.06$	$\lambda = 10.6$		$\lambda = 1.06$	$\lambda = 10.6$	
1.0	1.44(−40)	4.42(−40)	4.11	2.49(−40)	1.35(−39)	12.7	5.56(−40)	7.50(−39)	50.2
.8	1.87(−40)	6.63(−38)	3.04	4.71(−40)	1.04(−37)	4.44	1.54(−39)	3.06(−37)	11.4
.6	4.21(−40)	4.24(−37)	4.50	6.25(−40)	6.00(−37)	6.50	1.19(−39)	9.63(−37)	10.6
.4	1.18(−39)	1.02(−36)	4.41	1.60(−39)	1.45(−36)	6.44	1.83(−39)	2.12(−36)	9.34
.2	1.98(−39)	1.51(−36)	3.74	2.65(−39)	2.10(−36)	5.32	3.08(−39)	3.00(−36)	7.53
0	2.30(−39)	1.64(−36)	2.72	3.00(−39)	2.14(−36)	3.65	3.80(−39)	3.00(−36)	5.05
−.2	1.88(−39)	1.30(−36)	1.50	2.19(−39)	1.44(−36)	1.72	2.78(−39)	1.76(−36)	1.98
−.4	9.51(−40)	6.91(−37)	.556	6.76(−40)	4.51(−37)	.404	4.27(−40)	1.23(−37)	.0999
−.6	7.43(−40)	6.32(−37)	.420	8.45(−40)	8.44(−37)	.618	1.65(−39)	1.96(−36)	1.57
−.8	3.69(−39)	2.65(−36)	1.25	7.52(−39)	5.74(−36)	2.75	1.77(−38)	1.51(−35)	7.60
−1.0	1.36(−38)	9.04(−36)	3.83	2.84(−38)	1.98(−35)	8.41	6.84(−38)	5.19(−35)	22.7

* Integer in parenthesis is appropriate power of ten.

where v_e is incident electron velocity, j_p is incident photon flux, V_{ea} is the volume of intersection of the electron and atom beams, and V_{eap} is the volume of intersection of the electron, atom and photon beams.

Note from the table that $d\sigma_{ab}/d\Omega$ is small in the forward direction and sharply peaked in the backward direction, in contrast to the situation for elastic scattering. This can be qualitatively understood by the classical argument that forward-scattered electrons undergo minimum acceleration while the back-scattered ones undergo maximum acceleration, and the probability of emitting (or absorbing) radiation would vary directly with the magnitude of the acceleration experienced. If the electric polarization vector were taken parallel to the atom beam, $d\sigma_{ab}/d\Omega$ in the plane of the photon and incident electron beams would vanish. Consequently, a circularly polarized photon beam would give the same result in this plane (except for factor $\frac{1}{2}$) as we obtained for the original case of linear polarization.

(b) *Thermal averages*

The calculated thermally averaged absorption coefficients, as defined in (6), are given in Table 4 as a function of λ and TAYLOR and CALEDONIA[26] have extracted these cross sections for N, O, Ne, Ar and Xe from shock tube measurements. A comparison of their results and the present calculation is given in Table 5. Excellent agreement is obtained for Ne at 12,600°K and fair agreement for Xe at 8200°K, while for the other gases the calculated values are about a factor of 3 or 4 below the measurement. The experiments and their interpretation are difficult. Aside from the geometrical and stability problems in dealing with shock-heated gases, there are uncertainties in the concentrations of electrons, atoms, molecules (in the molecular gases) and ions. All other sources of continuum radiation must be accounted for in order to extract the desired neutral bremsstrahlung contribution.

MJOLSNESS and RUPPEL[11] have evaluated free–free emission coefficients as a function of photon energy for N and O for a few values of k_f^2. Their results for N range from about

TABLE 4. CALCULATED FREE–FREE ATOMIC ABSORPTION COEFFICIENTS PER UNIT ELECTRON DENSITY (IN cm^5)

λ (μm)	T(°K) 500	1000	2000	5000	10,000	15,000	20,000
			Helium				
0.5	2.21(−40)	2.31(−40)	2.52(−40)	3.20(−40)	4.39(−40)	5.60(−40)	6.79(−40)
1.0	5.91(−40)	6.55(−40)	7.94(−40)	1.26(−39)	2.14(−39)	3.06(−39)	3.99(−39)
2.0	1.71(−39)	2.10(−39)	2.99(−39)	6.22(−39)	1.27(−38)	1.97(−38)	2.70(−38)
5.0	8.48(−39)	1.30(−38)	2.40(−38)	6.80(−38)	1.62(−37)	2.68(−37)	3.79(−37)
10.0	3.51(−38)	6.53(−38)	1.44(−37)	4.76(−37)	1.21(−36)	2.05(−36)	2.93(−36)
15.0	8.87(−38)	1.83(−37)	4.37(−37)	1.54(−36)	3.99(−36)	6.81(−36)	9.77(−36)
20.0	1.78(−37)	3.94(−37)	9.81(−37)	3.56(−36)	9.34(−36)	1.60(−35)	2.30(−35)
			Carbon				
0.5	8.84(−41)	1.55(−40)	2.48(−40)	4.45(−40)	7.10(−40)	9.67(−40)	1.23(−39)
1.0	1.65(−40)	2.99(−40)	5.29(−40)	1.23(−39)	2.61(−39)	4.24(−39)	6.07(−39)
2.0	4.30(−40)	8.26(−40)	1.68(−39)	5.19(−39)	1.39(−38)	2.54(−38)	3.88(−38)
5.0	2.20(−39)	5.06(−39)	1.29(−38)	5.39(−38)	1.72(−37)	3.38(−37)	5.37(−37)
10.0	9.70(−39)	2.59(−38)	7.72(−38)	3.75(−37)	1.28(−36)	2.57(−36)	4.13(−36)
15.0	2.52(−38)	7.31(−38)	2.35(−37)	1.21(−36)	4.21(−36)	8.53(−36)	1.38(−35)
20.0	5.08(−38)	1.57(−37)	5.26(−37)	2.79(−36)	9.86(−36)	2.00(−35)	3.25(−35)

TABLE 4 (*cont.*)

λ (μm)	T(°K) 500	1000	2000	5000	10,000	15,000	20,000
				Nitrogen			
0.5	5.42(−41)	1.03(−40)	1.70(−40)	3.10(−40)	4.99(−40)	6.84(−40)	8.77(−40)
1.0	1.06(−40)	2.07(−40)	3.75(−39)	8.80(−40)	1.87(−39)	3.05(−39)	4.38(−39)
2.0	3.00(−40)	5.97(−40)	1.22(−39)	3.76(−39)	1.01(−38)	1.83(−38)	2.82(−38)
5.0	1.73(−39)	3.87(−39)	9.57(−39)	3.93(−38)	1.25(−37)	2.45(−37)	3.90(−37)
10.0	7.95(−39)	2.03(−38)	5.78(−38)	2.74(−37)	9.27(−37)	1.86(−36)	3.00(−36)
15.0	2.09(−38)	5.76(−38)	1.76(−37)	8.81(−37)	3.05(−36)	6.18(−36)	1.00(−35)
20.0	4.26(−38)	1.24(−37)	3.95(−37)	2.04(−36)	7.15(−36)	1.45(−35)	2.36(−35)
				Oxygen			
0.5	3.54(−41)	5.92(−41)	9.61(−41)	1.85(−40)	3.18(−40)	4.54(−40)	5.99(−40)
1.0	8.46(−41)	1.40(−40)	2.44(−40)	5.82(−40)	1.28(−39)	2.13(−39)	3.12(−39)
2.0	2.75(−40)	4.68(−40)	8.96(−40)	2.67(−39)	7.13(−39)	1.31(−38)	2.03(−38)
5.0	1.64(−39)	3.25(−39)	7.50(−39)	2.88(−38)	8.97(−38)	1.76(−37)	2.83(−37)
10.0	7.40(−39)	1.72(−38)	4.58(−38)	2.02(−37)	6.68(−37)	1.34(−36)	2.18(−36)
15.0	1.92(−38)	4.89(−38)	1.40(−37)	6.50(−37)	2.20(−36)	4.46(−36)	7.27(−36)
20.0	3.92(−38)	1.05(−37)	3.14(−37)	1.51(−36)	5.15(−36)	1.05(−35)	1.71(−35)
				Neon			
0.5	4.18(−41)	4.52(−41)	5.29(−41)	7.88(−41)	1.29(−40)	1.86(−40)	2.50(−40)
1.0	1.12(−40)	1.31(−40)	1.75(−40)	3.31(−40)	6.56(−40)	1.05(−39)	1.50(−39)
2.0	3.05(−40)	4.10(−40)	6.64(−40)	1.68(−39)	3.97(−39)	6.84(−39)	1.02(−38)
5.0	1.36(−39)	2.41(−39)	5.28(−39)	1.86(−38)	5.12(−38)	9.35(−38)	1.44(−37)
10.0	5.33(−39)	1.18(−38)	3.16(−38)	1.30(−37)	3.83(−37)	7.14(−37)	1.11(−36)
15.0	1.32(−38)	3.30(−38)	9.58(−38)	4.20(−37)	1.26(−36)	2.37(−36)	3.71(−36)
20.0	2.65(−38)	7.07(−38)	2.15(−37)	9.73(−37)	2.96(−36)	5.58(−36)	8.74(−36)
				Argon			
0.5	2.78(−41)	4.21(−41)	7.28(−41)	1.79(−40)	4.04(−40)	6.96(−40)	1.05(−39)
1.0	2.95(−41)	6.14(−41)	1.41(−40)	5.04(−40)	1.55(−39)	3.17(−39)	5.36(−39)
2.0	5.69(−41)	1.27(−40)	4.07(−40)	2.19(−39)	8.51(−39)	1.94(−38)	3.49(−38)
5.0	7.92(−40)	8.32(−40)	2.88(−39)	2.29(−38)	1.06(−37)	2.60(−37)	4.85(−37)
10.0	5.16(−39)	4.73(−39)	1.68(−38)	1.59(−37)	7.92(−37)	1.98(−36)	3.74(−36)
15.0	1.37(−38)	1.34(−38)	5.08(−38)	5.12(−37)	2.61(−36)	6.58(−36)	1.25(−35)
20.0	2.57(−38)	2.81(−38)	1.13(−37)	1.19(−36)	6.11(−36)	1.55(−35)	2.94(−35)
				Krypton			
0.5	2.21(−41)	4.78(−41)	1.02(−40)	2.85(−40)	6.58(−40)	1.10(−39)	1.58(−39)
1.0	9.57(−41)	9.11(−41)	1.50(−40)	6.22(−40)	2.22(−39)	4.68(−39)	7.73(−39)
2.0	1.08(−39)	7.22(−40)	6.12(−40)	2.39(−39)	1.16(−38)	2.79(−38)	4.95(−38)
5.0	1.29(−38)	8.93(−39)	6.53(−39)	2.40(−38)	1.42(−37)	3.71(−37)	6.85(−37)
10.0	6.78(−38)	5.26(−38)	4.13(−38)	1.65(−37)	1.06(−36)	2.82(−36)	5.28(−36)
15.0	1.75(−37)	1.50(−37)	1.25(−37)	5.31(−37)	3.47(−36)	9.36(−36)	1.76(−35)
20.0	3.43(−37)	3.19(−37)	2.80(−37)	1.23(−36)	8.13(−36)	2.20(−35)	4.14(−35)
				Xenon			
0.5	6.76(−41)	1.42(−40)	2.89(−40)	7.27(−40)	1.47(−39)	2.18(−39)	2.80(−39)
1.0	3.11(−40)	2.54(−40)	3.57(−40)	1.37(−39)	4.63(−39)	8.95(−39)	1.34(−38)
2.0	3.70(−39)	2.31(−39)	1.63(−39)	4.93(−39)	2.33(−38)	5.24(−38)	8.51(−38)
5.0	4.64(−38)	3.07(−38)	2.03(−38)	4.95(−38)	2.84(−37)	6.92(−37)	1.17(−36)
10.0	2.41(−37)	1.80(−37)	1.31(−37)	3.42(−37)	2.10(−36)	5.26(−36)	9.04(−36)
15.0	6.13(−37)	5.09(−37)	3.99(−37)	1.10(−36)	6.92(−36)	1.75(−35)	3.01(−35)
20.0	1.19(−36)	1.08(−36)	8.92(−37)	2.54(−36)	1.62(−35)	4.11(−35)	7.10(−35)

TABLE 5. COMPARISON OF MEASUREMENTS OF TAYLOR AND CALEDONIA AND PRESENT CALCULATION FOR FREE–FREE ATOMIC ABSORPTION COEFFICIENT PER UNIT ELECTRON DENSITY (IN cm^5)

Atom	T(°K)	$\lambda(\mu m)$	Present calculation	Taylor and Caledonia
N	9175	2.0	8.86(−39)	3.20(−38)
		3.5	3.97(−38)	1.30(−37)
		5.0	1.08(−37)	3.00(−37)
O	9700	2.0	6.82(−39)	2.90(−38)
		3.5	3.12(−38)	1.00(−37)
		5.0	8.53(−38)	2.60(−37)
Ne	12,600	2.0	5.40(−39)	5.80(−39)
		3.5	2.59(−38)	2.70(−38)
		5.0	7.21(−38)	7.20(−38)
Ar	9900	2.0	8.34(−39)	3.80(−38)
		3.5	3.81(−38)	1.50(−37)
		5.0	1.04(−37)	3.60(−37)
Xe	8200	2.0	1.51(−38)	3.00(−38)
		3.5	6.50(−38)	9.60(−38)
		5.0	1.74(−37)	2.00(−37)

40 per cent below the present values for 5 eV electron energy to about 10 per cent above the present values for 1 eV electron energy. For O, their results are about 15 per cent below the present values for 5 eV electron energy and about 20 per cent above the present values for 1 eV electron energy. These difficulties are attributable to the differences in the atomic models and potentials used.

Some calculations have been done on the free–free absorption of He^- and Ne^- by MCDOWELL *et al.*[27,28] using an asymptotic approximation. Their results for He^- in the range $\lambda = 0.5$–$1.0\ \mu m$ and $T = 5000$–$10{,}000$°K are about 30 per cent below our present results, but their results for Ne^- are between a factor of a 100–1000 larger than our present results. We interpret this as further evidence of the undependability of asymptotic approximations in the case of heavier atoms. JOHN[29] obtained a slight modification from McDowell *et al.* in the He^- result when using somewhat different phase shifts in an asymptotic approximation. The results of MYERSCOUGH and MCDOWELL[30] for C^- in an asymptotic approximation are larger than the present results by a factor of about 2–7 in the above range of λ and T.

The corresponding emissivities can be simply obtained from Table 4 and the definitions in equations (5)–(8). The formula

$$J(\lambda, T) = \frac{1.19 \times 10^4}{\lambda^5} e^{-(1.439 \times 10^4/\lambda T)} \kappa(\lambda, T), \tag{14}$$

gives the volume emissivity in units of W per cm^3 per μm per steradian, when λ is expressed in μm, T in °K, and κ is the absorption coefficient in Table 4. In other words, the bremsstrahlung power per micron radiated into unit solid angle by a volume V cm^3 of hot gas is equal to $n_e n_a V J$ W, where n_e and n_a are the electron and atom number densities. We have omitted the stimulated emission factor, $1 - e^{-\hbar\omega/kT}$, from all absorption coefficients tabulated in this paper.

We estimate an absolute uncertainty of about 30 per cent in our presently calculated values. This estimate is based upon the following considerations.

(a) For every atom for which reliable total elastic and momentum transport cross sections are available our calculated fits as given in Table 2 are generally within the experimental scatter. This applies also to the Ramsauer region as well as to differential cross sections, indicating that our individual partial waves are accurate as well as their summed result.

(b) In the two cases for which photodetachment measurements are available, i.e. for C and O, our present model potential produces cross sections which are within 30 per cent of experiment.[14] The largest part of this error is expected to arise from inaccuracies in the bound wave function, which is more influenced by correlation and exchange effects than are the continuum wave functions.

(c) The continuum wave functions which enter into the free–free absorption coefficient in the temperature range here considered correspond to energies which are too low for the existence of Feshbach or core-excited resonances. Such resonances are not representable by our present atomic model, but the lower energy 'shape resonances' are.

(d) Comparison of our present model with the more detailed calculations for hydrogen support the above estimated uncertainty. This is discussed in detail in the following section.

(c) *Comparison with detailed hydrogen calculations*

As mentioned previously, the astrophysical interest in the free–free absorption of an electron in the field of a hydrogen atom has stimulated much work on this system. Also, of course, the fact that it is only a two electron system allows for a more complete theoretical treatment than is possible for more complex atoms. The low energy elastic scattering of electrons by hydrogen has been treated exhaustively by variational and close-coupling methods, in which correlation and exchange effects between the two electrons are accounted for. Using the two-electron singlet and triplet scattering wave functions, the two-electron dipole matrix elements have been evaluated and their squares statistically averaged. The free–free absorption coefficient for the H^- system has been thus evaluated by GELTMAN[6] using variational wave functions containing 6 linear parameters, by JOHN[7] in the exchange-polarization approximation, and by DOUGHTY and FRASER[8] using $1s$–$2s$ close-coupling wave functions. We would like to compare the results of these very elaborate calculations with the results which follow from our present atomic model.

The static potential presented by a frozen ground-state hydrogen atom to a free electron is the well known function $-2\,e^{-2r}(1+1/r)$. When polarization is allowed for, the effective potential takes the form

$$U_{\text{hyd}}(r) = -2\,e^{-2r}\left(1+\frac{1}{r}\right) - \alpha\frac{(1-e^{-r/r_p})}{(r_p^2+r^2)^2}. \tag{15}$$

Our first term here takes the place of the first two terms in (12), or $U_{HS} = -(2/r)(1+r\,e^{-2r})$ and $r_0 = \frac{1}{2}$. The polarizability of hydrogen is known exactly ($\alpha = 4.5\,a_0^3$) and we are left with one parameter, r_p, to adjust for a fit to the known elastic scattering cross section. This latter quality is known to high accuracy, not from experiment, but from very precise variational calculations.[31–33] We find that the model potential (15) yields an elastic scattering cross section for $E < 10\,\text{eV}$ which lies within 10 per cent of the "exact" one when $r_p = 1.125\,a_0$.

Having optimized our model potential for the electron-hydrogen system, we then calculate the free–free absorption coefficient in exactly the same manner as for all the other atoms presently considered. The results are compared with those of the more elaborate calculations in Table 6. The results of the more elaborate calculations are given in units of $cm^2/(dyne/cm^2)$ (i.e. per unit electron pressure) and also contain the stimulated emission factor. Thus they must be multiplied by $6.96 \times 10^{-13}\theta^{-1}(1-e^{-31.320\Delta k^2})^{-1}$ to be converted into our present units of cm^5/unit electron density ($\theta = 5040/T$). We note that the agreement in all cases is no worse than the order of 30 per cent, and often better. The worst possible case for the representation of an electron–atom interaction as a static potential should be hydrogen. Correlation and exchange effects should decrease in relative importance as the atomic number is increased and the incoming electron sees a more statistical smear of bound electrons. For this reason we expect the uncertainty of our model in the case of hydrogen to be in the nature of an upper bound when the model is extended to the heavier atoms of Table 4.

TABLE 6. FREE–FREE ABSORPTION COEFFICIENT PER UNIT ELECTRON DENSITY FOR HYDROGEN (IN 10^{-39} cm^5)

T(°K)	$\lambda(\mu m)$	Geltman(6)	John(7)	Doughty and Fraser(8)	Present
	0.456	1.21	1.45	1.36	1.07
2520	0.911	4.81	3.84	4.18	3.61
	1.519	11.2	9.48	10.8	9.64
	0.456	1.25	1.31	1.29	1.08
4200	0.911	4.80	4.06	4.35	4.03
	1.519	12.8	11.3	12.4	11.9
	0.456	1.53	1.22	1.22	1.12
8400	0.911	5.53	4.79	4.97	4.95
	1.519	17.0	15.8	16.4	16.9

Acknowledgments—I would like to thank Drs. A. V. PHELPS, L. J. KIEFFER and J. W. COOPER for many helpful discussions, and H. ODABASI for supplying decks of the Herman–Skillman potential. I'm greatly indebted to URSULA PALMER for having done all the coding, code-checking, and computer runs needed in this work. This research was supported in part by the Advanced Research Projects Agency of the Department of Defense and was monitored by U.S. Army Research Office-Durham, under Contract No. DAHCO4 72 C 0047.

RFERENCES

1. A. SOMMERFELD and A. MAUE, *Ann. Phys.* **23,** 589 (1935).
2. D. H. MENZEL and C. L. PEKERIS, *Mon. Not. R. Astr. Soc.* **96,** 77 (1935).
3. G. PEACH, *Mem. R. Astr. Soc.* **71,** 1 (1967).
4. S. CHANDRASEKHAR and F. H. BREEN, *Astrophys. J.* **104,** 430 (1946).
5. T. OHMURA, *Astrophys. J.* **140,** 282 (1964).
6. S. GELTMAN, *Astrophys. J.* **141,** 376 (1965).
7. T. L. JOHN, *Mon. Not. R. Astr. Soc.* **131,** 315 (1966).
8. N. A. DOUGHTY and P. A. FRASER, *Mon. Not. R. Astr. Soc.* **132,** 267 (1966).
9. R. V. DEVORE, *Phys. Rev.* **136,** A666 (1964); **140,** AB3 (1965).
10. B. KIVEL, *JQSRT* **7,** 27 (1967).
11. R. C. MJOLSNESS and H. M. RUPPEL, *Phys. Rev.* **154,** 98 (1967).
12. L. M. BIBERMAN and G. E. NORMAN, *Sov. Phys. Uspekhi* **10,** 52 (1967).
13. V. P. MYERSCOUGH and G. PEACH, *Case Studies in Atomic Collision Physics*, Vol. 2, Chapt. 5, p. 293. North-Holland, Amsterdam (1972).

14. J. W. Cooper and J. B. Martin, *Phys. Rev.* **126,** 1482 (1962).
15. E. J. Robinson and S. Geltman, *Phys. Rev.* **153,** 4 (1967).
16. F. Herman and S. Skillman, *Atomic Structure Calculations*. Prentice-Hall, Englewood Cliffs, New Jersey (1963).
17. R. R. Teachout and R. L. Pack, *Atomic Data* **3,** 195 (1971).
18. L. J. Kieffer, *Atomic Data* **2,** 293 (1971).
19. G. Sunshine, B. B. Aubrey and B. Bederson, *Phys. Rev.* **154,** 1 (1967).
20. R. Neynaber, E. W. Rothe, L. L. Marino and S. M. Trujillo, *Phys. Rev.* **123,** 148 (1961).
21. F. E. Low, *Phys. Rev.* **110,** 974 (1958).
22. M. Ashkin, *Phys. Rev.* **141,** 41 (1966).
23. R. R. Johnston, *JQSRT* **7,** 815 (1967).
24. R. C. Mjolsness and H. M. Ruppel, *Phys. Rev.* **186,** 83 (1969).
25. H. Ehrhardt, private communication.
26. R. L. Taylor and G. Caledonia, *JQSRT* **9,** 657; 681 (1969).
27. M. R. C. McDowell, J. H. Williamson and V. P. Myerscough, *Astrophys. J.* **144,** 827 (1966).
28. M. R. C. McDowell, *Observatory* **91,** 217 (1971).
29. T. L. John, *Mon. Not. R. Astr. Soc.* **138,** 137 (1968).
30. V. P. Myerscough and M. R. C. McDowell, *Mon. Not. R. Astr. Soc.* **132,** 457 (1966).
31. C. Schwartz, *Phys. Rev.* **124,** 1468 (1961).
32. R. L. Armstead, *Phys. Rev.* **171,** 91 (1968).
33. M. K. Gailitis, *Atomic Collisions*, Vol. 3. (Latvian Academy of Sciences) 155 (1965).